Stoichiometry of Transjunctional Voltage–gating Polarity Reversal by a Negative Charge Substitution in the Amino Terminus of a Connexin32 Chimera

Seunghoon Oh, Charles K. Abrams, Vytas K. Verselis, and Thaddeus A. Bargiello

From the Department of Neuroscience, Albert Einstein College of Medicine, Bronx, New York, 10461

abstract Gap junctions are intercellular channels formed by the serial, head to head arrangement of two hemichannels. Each hemichannel is an oligomer of six protein subunits, which in vertebrates are encoded by the connexin gene family. All intercellular channels formed by connexins are sensitive to the relative difference in the membrane potential between coupled cells, the transjunctional voltage (V_j), and gate by the separate action of their component hemichannels (Harris, A.L., D.C. Spray, and M.V. Bennett. 1981. *J. Gen. Physiol.* 77:95–117). We reported previously that the polarity of V_j dependence is opposite for hemichannels formed by two closely related connexins, Cx32 and Cx26, when they are paired to form intercellular channels (Verselis, V.K., C.S. Ginter, and T.A. Bargiello. 1994. *Nature.* 368:348–351). The opposite gating polarity is due to a difference in the charge of the second amino acid. Negative charge substitutions of the neutral asparagine residue present in wild-type Cx32 (Cx32N2E or Cx32N2D) reverse the gating polarity of Cx32 hemichannels from closure at negative V_j to closure at positive V_j. In this paper, we further examine the mechanism of polarity reversal by determining the gating polarity of a chimeric connexin, in which the first extracellular loop (E1) of Cx32 is replaced with that of Cx43 (Cx43E1). The resulting chimera, Cx32*Cx43E1, forms conductive hemichannels when expressed in single *Xenopus* oocytes and intercellular channels in pairs of oocytes (Pfahnl, A., X.W. Zhou, R. Werner, and G. Dahl. 1997. *Pflügers Arch.* 433:733–779). We demonstrate that the polarity of V_j dependence of Cx32*Cx43E1 hemichannels in intercellular pairings is the same as that of wild-type Cx32 hemichannels and is reversed by the N2E substitution. In records of single intercellular channels, V_j dependence is characterized by gating transitions between fully open and subconductance levels. Comparable transitions are observed in Cx32*Cx43E1 conductive hemichannels at negative membrane potentials and the polarity of these transitions is reversed by the N2E substitution. We conclude that the mechanism of V_j dependence of intercellular channels is conserved in conductive hemichannels and term the process V_j gating. Heteromeric conductive hemichannels comprised of Cx32*Cx43E1 and Cx32N2E*Cx43E1 subunits display bipolar V_j gating, closing to substates at both positive and negative membrane potentials. The number of bipolar hemichannels observed in cells expressing mixtures of the two connexin subunits coincides with the number of hemichannels that are expected to contain a single oppositely charged subunit. We conclude that the movement of the voltage sensor in a single connexin subunit is sufficient to initiate V_j gating. We further suggest that V_j gating results from conformational changes in individual connexin subunits rather than by a concerted change in the conformation of all six subunits.

key words: ion channels • voltage dependence • bipolar gating • gating mechanisms • gap junction

INTRODUCTION

Gap junctions are intercellular channels formed by the interaction of two hemichannels or connexins. Each hemichannel is composed of six protein subunits, connexins, which surround a central aqueous pore with a radius of ~7 Å (Veenstra, 1996; Oh et al., 1997). The three-dimensional structure of a Cx43 gap junction channel solved at ~7 Å resolution (Unger et al., 1999) has confirmed the essential features of the membrane topology of connexins determined biochemically (see Zimmer et al., 1987; Hertzberg et al., 1988; Milks et al., 1988). Each connexin subunit spans the membrane four times (TM1–TM4) and has intracellular NH_2 and COOH termini. Two extracellular loops (E1 and E2)[1] interact to form the complete intercellular channel. The 3-D structure revealed that the portion of the channel pore that spans the membrane bilayer is formed by two different transmembrane helices (Unger et al., 1999), which we have proposed to be transmembranes 1 and 2 (TM1 and TM2) (Ri et al., 1999).

All intercellular channels formed by the 16 members of the vertebrate connexin gene family are sensitive to the difference in membrane potential between coupled cells, the transjunctional voltage (V_j), while some also display weak sensitivity to the absolute membrane potential (V_m) (see Verselis et al., 1991). Transjunctional voltage dependence (V_j dependence) is essentially a hemichannel property, although its expression may be modified by hemichannel interactions (Harris et al., 1981; Verselis et al., 1994). Each hemichannel is be-

Address correspondence to Dr. T.A. Bargiello, Department of Neuroscience, Kennedy Center, Albert Einstein College of Medicine, 1410 Pelham Parkway South, Bronx, NY 10461. Fax: 718-430-8821; E-mail: bargiell@aecom.yu.edu.

[1]*Abbreviations used in this paper:* E1, first extracellular loop; TM1, first transmembrane segment; V_j, transjunctional voltage.

lieved to contain a separate voltage sensor and gate, whose formation does not depend upon protein interactions arising from pairing. The transjunctional voltage sensor most likely lies within and close to the cytoplasmic entrance of the channel pore, since in this position it can sense the difference between the membrane potentials of coupled cells (V_j) while being largely insensitive to changes in the absolute membrane potential of either cell (V_m or $V_{i\text{-}o}$).

We have reported that the polarity of V_j dependence is opposite in hemichannels formed by Cx32 and Cx26 when they are paired to form intercellular channels (Verselis et al., 1994; Oh et al., 1999). The opposite gating polarity is due to a difference in the charge of the second amino acid of the two connexins. The substitution of the neutral asparagine (N2) residue present in Cx32 with negatively charged residues (either Cx32N2D or N2E) reverses the negative gating polarity of wild-type Cx32 hemichannel V_j dependence. Similarly, the substitution of the negatively charged D2 residue present in wild-type Cx26 with neutral or positively charged residues reverses the positive gating polarity of Cx26 homomeric hemichannels. The relation between the charge of amino acids in the amino terminus and the polarity of the applied V_j indicates that the overall mechanism of V_j gating is conserved. Closure of homomeric hemichannels formed by either Cx32 or Cx26 would result from or be initiated by the movement of the amino terminus towards the cytoplasm of the cell.

While negative charge substitutions up to and including the 10th amino acid residue can reverse the V_j-gating polarity of Cx32 hemichannels (Purnick, Oh, Abrams, Verselis, and Bargiello, manuscript submitted for publication), a negative charge substitution of the 11th amino acid residue (Cx32S11D) cannot. Taken together, these results indicate that the first 10 amino acid residues can reside within the transjunctional electric field and that charged residues at any of these positions can contribute to the formation of the transjunctional voltage sensor. We have recently shown that the inherent structural flexibility of a glycine residue (G12), conserved in Group I (β) connexins, allows the formation of a turn, which positions the amino terminus within the channel pore (Purnick, Benjamin, Verselis, Barhgiello, and Dowd, manuscript submitted for publication). It should be noted that there is no evidence for a comparable turn in the NH_2 terminus of Group II (α) connexins, although D3N appears to reverse the gating polarity of Cx46 hemichannels (Verselis, V.K., unpublished observation).

Hemichannels formed by some connexins including Cx46, Cx56, a Cx32 chimera designated Cx32*Cx43E1, and perhaps Cx32 form voltage-dependent conductive hemichannels when they are unapposed by a hemichannel expressed in a second cell (Paul et al., 1991; Ebihara et al., 1995; Ebihara, 1996; Trexler et al., 1996; Castro et al., 1999). Conductive hemichannels formed by Cx46 display at least two distinct forms of voltage dependence, "V_j gating" and "loop gating" (see Trexler et al., 1996). The term V_j gating was used by Trexler et al. (1996) to convey the likelihood of a similarity in the mechanism of voltage dependence of Cx46 conductive hemichannels at positive membrane potentials to the gating of Cx46 intercellular channels in response to V_j. As discussed later in this paper, V_j gating in Cx32 is related to conformational changes initiated by, or resulting from, the movement of the amino terminus of the constituent connexin subunits. The second gating mechanism, termed loop gating was used to describe the gating of Cx46 conductive hemichannels at negative membrane potentials. Loop gating is characterized by a reversible series of stepwise changes in conductance that give the appearance of "slow" gating transitions that often result in complete channel openings and closings. Similar-appearing slow gating transitions are observed in single-channel recordings of intercellular channels (see Neyton and Trautmann, 1985; Bukauskas and Weingart, 1994; Oh et al., 1997) and in single-channel studies of "chemical" gating of both intercellular and conductive hemichannels by Ca^{2+} and H^+ (Bukauskas and Peracchia, 1997; Trexler et al., 1999). It is not known if all these "slow" gating transitions share a common set of molecular determinants, but this is a reasonable possibility.

In this paper, we explore further the mechanistic and structural correlates of voltage-dependent gating of channels formed by Cx32 by determining the stoichiometry of polarity reversal by the N2E substitution. As these experiments are difficult, if not impossible, to accomplish with intercellular channels, we examined the gating polarity of conductive heteromeric hemichannels formed by expressing mixtures of Cx32*Cx43E1 and Cx32N2E*Cx43E1 in *Xenopus* oocytes. We demonstrate that heteromeric conductive hemichannels, containing subunits with either positive or negative charges in their NH_2 termini, exhibit bipolar V_j gating. The frequency of bipolar hemichannels observed correlates with the fraction of hemichannels that are expected to contain at least one oppositely charged connexin subunit. Therefore, the movement of the voltage sensor in a single connexin subunit is sufficient to initiate V_j gating. We propose that channel closure also results from a conformational change in individual connexin subunits rather than by a concerted change in the conformation of all six subunits.

MATERIALS AND METHODS

Construction of Chimeric Connexins, RNA Synthesis, and Oocyte Injection

A Cx32 chimera, Cx32*Cx43E1, in which the first extracellular loop (E1, residues E41–R75) of Cx32 is replaced by the corre-

sponding segment of Cx43 (residues E42–R76) was made using oligonucleotide primers with the polymerase chain reaction. For Cx32N2E*Cx43E1, the DNA segment containing the N2E substitution was excised by restriction enzymes and subcloned into Cx32*Cx43E1. Both chimeric connexins were cloned into the plasmid vector, pGem-7zf(+) (Promega) and sequenced in entirety. RNA was synthesized from linearized plasmid templates using a "mMESSAGE mMACHINE" T7 Kit (Ambion) according to the manufacturer's protocol. For the subunit stoichiometry experiments, DNA concentrations were determined spectrophotometrically and mixed in appropriate ratios before RNA synthesis.

Approximately 50 nl of 1 ng/nl RNA was coinjected into a *Xenopus* oocyte with 0.3 pmol/nl of an antisense phosphorothioate oligonucleotide complimentary to *Xenopus* Cx38. This antisense oligonucleotide blocks all endogenous coupling between oocyte pairs attributable to Cx38 within 72 h (Barrio et al., 1991; Rubin et al., 1992). After RNA injection, oocytes were kept in a bath solution, ND96, containing (mM): 88 NaCl, 1 KCl, 5 $CaCl_2$, 1 $MgCl_2$, 10 HEPES, 0.1% glucose, and 2.5 pyruvate, pH 7.6. Oocytes were devitellinized in a hypertonic solution containing (mM): 220 Na aspartate, 10 KCl, 2 $MgCl_2$, and 10 HEPES, pH 7.6.

Electrophysiological Recordings

Macroscopic recordings from pairs of *Xenopus* oocytes were performed and data were analyzed as described by Rubin et al. (1992) and Verselis et al. (1994).

Voltage-clamp recordings of macroscopic currents from single *Xenopus* oocytes were obtained with a two-electrode voltage clamp (GeneClamp 500; Axon Instruments, Inc.). Electrodes were filled with 2 M KCl. Data were acquired using pClamp 6.0 software and a Digidata 1200 interface (Axon Instruments, Inc.).

In all patch-clamp experiments, the pipette solution was same as a bath solution described above, except $CaCl_2$ and $MgCl_2$ were replaced by 2 mM EDTA and 2 mM EGTA (ND98). Single channel data were acquired using pClamp 7.0 software, an Axopatch 200B integrating patch amplifier, and a Digidata 1200A interface (Axon Instruments, Inc.). Data were acquired at 5 kHz and filtered at 1 kHz with a four-pole low pass Bessel filter.

RESULTS

*Polarity of V_j Gating of Cx32*Cx43E1 and Cx32N2E*Cx43E1 Hemichannels Inferred from the Voltage Dependence of Intercellular Channels*

A Cx32 chimera, Cx32*Cx43E1, in which the first extracellular loop (E1, residues E41–R75) of Cx32 is replaced by the corresponding segment of Cx43 (residues E42–R76) forms both conductive hemichannels and intercellular channels in *Xenopus* oocytes. The amino acid sequence of E1 differs by nine residues in the two connexins, and although four of the differences involve charged amino acid residues, there is no change in the net charge of the E1 loop.

We first examine whether the Cx43E1 substitution changes the gating polarity of Cx32 hemichannels or the ability of the N2E substitution to reverse the gating polarity of Cx32 hemichannels when they are paired to form intercellular channels. The data shown below demonstrates that the Cx43E1 substitution does not reverse the gating polarity of the Cx32 hemichannel, nor does it alter the ability of the N2E substitution to reverse the polarity of V_j dependence.

The conductance–voltage relations of heterotypic Cx32*Cx43E1/Cx32 and Cx32*Cx43E1/Cx26 junctions and homotypic Cx32*Cx43E1 junctions are shown in Fig. 1, A–C. In heterotypic pairings with Cx32, junctional currents decline to steady state levels for either polarity of V_j (Fig. 1 A), resembling those of homotypic Cx32 junctions (see Verselis et al., 1994; Oh et al., 1999) when the Cx32 side of the heterotypic junction is hyperpolarized or when the Cx32*Cx43E1 side is depolarized. In both cases, the difference in membrane potential creates a V_j such that the cytoplasmic face of the Cx32 hemichannel is negative with respect to the cytoplasmic face of the Cx32*Cx43E1 hemichannel. When the Cx32 side of the junction is relatively positive (the Cx32*Cx43E1 hemichannel relatively negative), junctional currents also decline, but at larger V_js and with substantially slower kinetics. These results indicate that the polarities of Cx32 and Cx32*Cx43E1 V_j dependence are the same; both close at negative transjunctional voltages.

In heterotypic pairings with Cx26, junctional conductance decreases to a minimum when the cell expressing Cx26 is relatively positive (Fig. 1 B). The voltage dependence of Cx32*Cx43E1/Cx26 junctions is qualitatively similar to that of heterotypic Cx32/Cx26 junctions. We conclude that Cx32*Cx43E1 and Cx26 hemichannels have opposite gating polarities. Thus, the asymmetry in the steady state conductance–voltage relation of the Cx32*Cx43E1/Cx26 junction is due to the closure of both V_j gates when the Cx26 cell is relatively positive and the opening of both V_j gates when the Cx26 cell is made relatively negative.

The conductance–voltage relation of initial currents of the Cx32*Cx43E1/Cx26 heterotypic junction is asymmetric and comparable with that of Cx32/Cx26 heterotypic channels. The voltage dependence of initial conductance reflects the rectification of open-channel currents and is a consequence of asymmetries in the position of charged residues that result from the heterotypic pairing (see Oh et al., 1999).

Junctional currents of homotypic Cx32*Cx43E1 intercellular channels decrease for either polarity of V_j, but do so asymmetrically. Currents decrease more when either cell is hyperpolarized to the same voltage (Fig. 1 C). In experimental paradigms in which the membrane potentials of both cells are changed equally and simultaneously, junctional conductance decreases when the cells are hyperpolarized and increases when they are depolarized (not shown). This result is consistent with the presence of V_m dependence. Although in this case, "chemical gating" may also contribute to the observed asymmetry in the conductance–voltage relation, as it is possible that the intercellular channel is gated by the voltage-dependent entry of Ca^{2+} (see Laz-

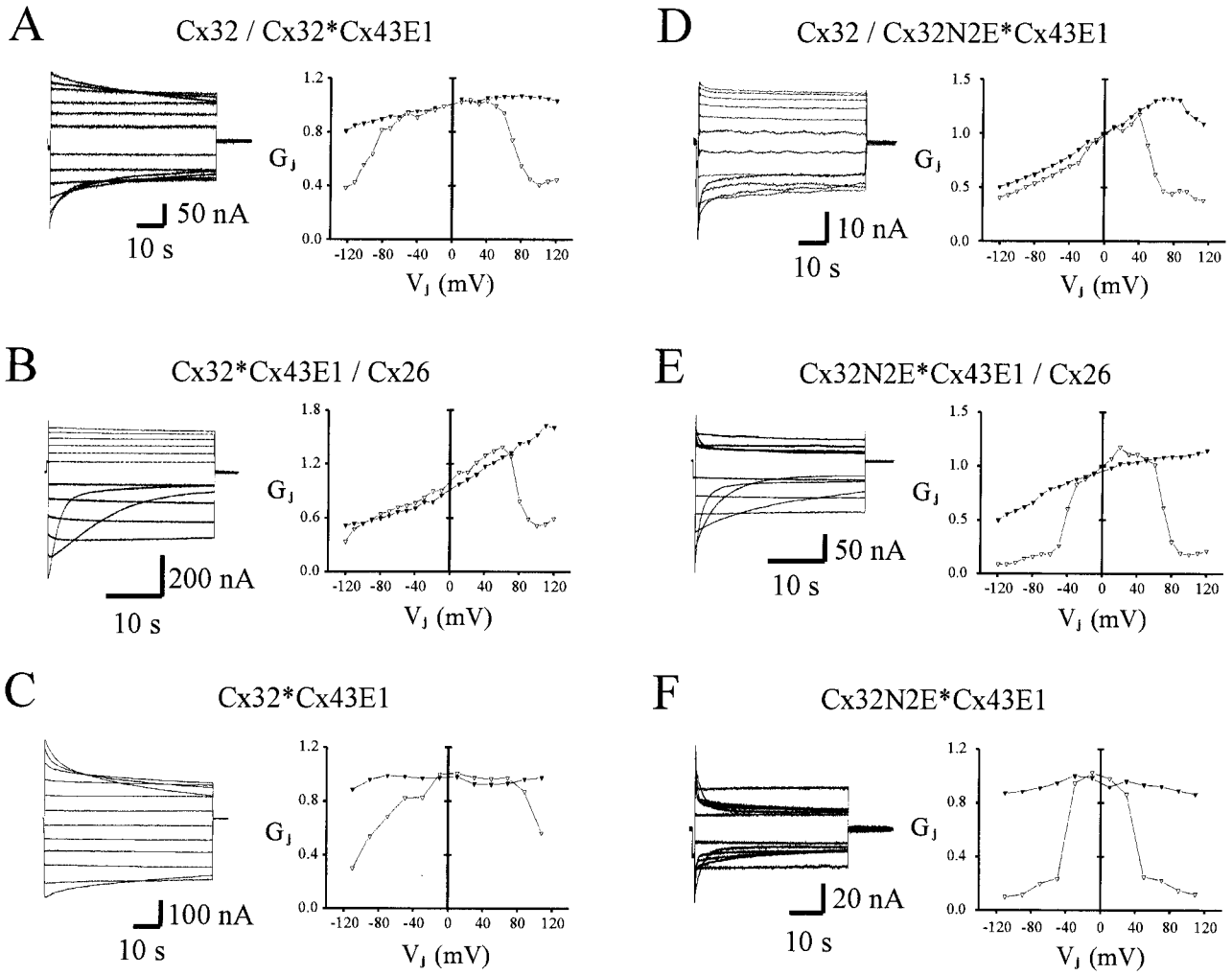

Figure 1. Representative conductance–voltage relations and macroscopic current traces of intercellular channels formed by the designated wild-type and chimeric connexins expressed in pairs of *Xenopus* oocytes. In all cases, junctional conductance is normalized to $V_j = 0$. Positive V_j is relative to the cytoplasmic entrance of the hemichannel appearing on the right side of the channel designation. Initial conductance is depicted by ▼, steady state conductance by ▽.

ark and Peracchia, 1993) through conductive hemichannels formed the Cx32*Cx43E1 chimera. In contrast, heterotypic Cx32/Cx32*Cx43E1 and Cx26/Cx32*Cx43E1 junctions are largely insensitive to V_m (not shown). This suggests that the presence of V_m dependence is sensitive to hemichannel pairing. V_m dependence is likely to be sensitive to hemichannel interactions, as the V_m sensor is expected to be located in the region of the extracellular gap and subject to interactions among the extracellular loops of the two hemichannels (see Verselis et al., 1991).

We next examined whether the N2E substitution reverses the gating polarity of Cx32*Cx43E1 hemichannels when they are paired to form intercellular channels. Negative charge substitutions at this position, Cx32N2E and Cx32N2D, reverse the gating polarity of Cx32 hemichannels, from closure at negative V_j to closure at positive V_j (Verselis et al., 1994; Oh et al., 1999).

The conductance–voltage relations of homotypic and heterotypic Cx32N2E*Cx43E1 junctions paired with Cx26 and Cx32 are shown in Fig. 1, D–F. Junctional currents in the Cx32N2E*Cx43E1/Cx32 heterotypic junction decline to steady state levels only when positive V_j is applied to the Cx32N2E*Cx43E1 side of the junction, the Cx32 side of the junction is relatively negative; whereas, in the Cx32N2E*Cx43E1/Cx26 heterotypic junction, steady state currents decline for both polarities of applied V_j. These results are opposite those obtained with heterotypic pairings of the parental Cx32*Cx43E1 junction. The asymmetry in the steady state conductance–voltage relation of the Cx32/Cx32N2E*Cx43E1 heterotypic junction qualitatively resembles that of the Cx32*Cx43E1/Cx26 junction, while the steady state conductance–voltage relation of Cx32N2E*Cx43E1/Cx26 qualitatively resembles that of the Cx32*Cx43E1/Cx32 heterotypic junction (compare Fig. 1, A, B, D, and E). These results indicate

that the negative charge substitution (N2E) reverses the gating polarity of V_j dependence in the Cx32*Cx43E1 hemichannel as it does in the wild-type Cx32 hemichannel. Closure of the Cx32N2E*Cx43E1 hemichannel occurs at smaller V_j and opposite polarity than the Cx32*Cx43E1 hemichannel. The N2E substitution also shifts the steady state conductance–voltage relation of the wild-type Cx32 channel (see Oh et al., 1999). The steady state conductance–voltage relation of the Cx32N2E*Cx43E1 homotypic junction is essentially symmetric, unlike that of the parental junction (compare Fig. 1, C and F). The symmetry can be explained if the increased sensitivity to V_j "masks" the less pronounced V_m dependence that is conferred by the Cx43E1 substitution.

*Voltage Dependence and Gating Polarity of Cx32*Cx43E1 and Cx32N2E*Cx43E1 Conductive Hemichannels*

Macroscopic recordings. A macroscopic recording of membrane currents in a *Xenopus* oocyte injected with Cx32*Cx43E1 RNA is presented in Fig. 2 A. Depolarizations of the oocyte membrane to positive potentials from a holding potential of −90 mV result in a slowly developing outward current that does not plateau during the 30-s voltage step. Depolarization of oocyte membranes to voltages greater than +40 mV in Ca^{2+} containing bath solutions usually leads to the activation of substantial outward endogenous currents (probably Ca^{2+}-activated Cl^- currents). These endogenous currents can obscure those attributable to the activation of the Cx32*Cx43E1 conductive hemichannel (not shown).

Tail currents resulting from the repolarization of the oocyte membrane to the initial holding potential of −90 mV exhibit a complex time course. Typically, tail currents show an initial increase and then slowly return to steady state levels with a multiexponential time course (Fig. 2 A). The time course of tail current relaxations is influenced by the concentration of Ca^{2+} in the bath solution. Reductions in Ca^{2+} concentration from 5 to 2 mM prolong the time required to reach steady state

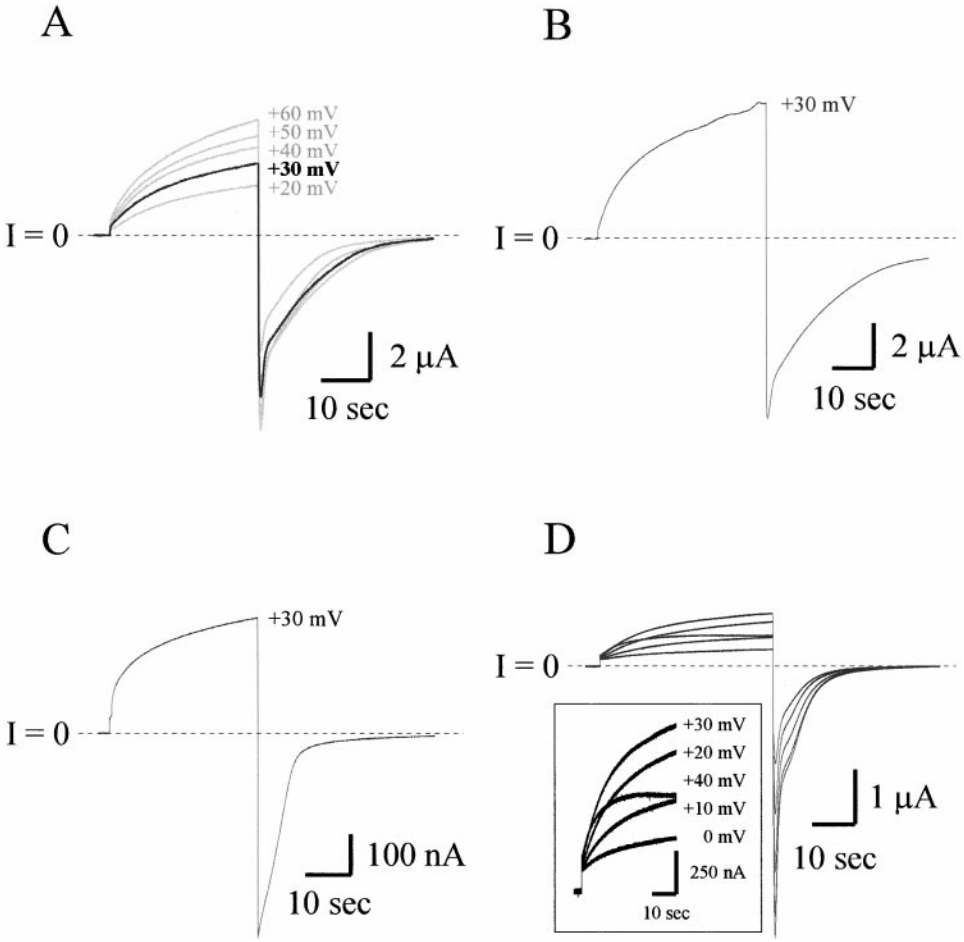

Figure 2. Macroscopic recordings of *Xenopus* oocytes expressing Cx32*Cx43E1 and Cx32N2E*Cx43E1 conductive hemichannels. (A) Outward currents in oocytes expressing Cx32*Cx43E1 were elicited from a holding potential at −90 mV, with 30-s voltage steps ranging from +20 to +60 mV in 10-mV increments. Inward tail currents resulted from the repolarization of the membrane to −90 mV. In 5 mM Ca^{2+}-containing bath solution, tail currents show an initial increase followed by a slow return to base line with a multiexponential time course. (B) The time course of the tail current relaxations is prolonged by reductions in the Ca^{2+} concentration of the bath solution from 5 to 2 mM. (C) Tail currents elicited by repolarization of the membrane to −90 mV in bath solutions containing 2 mM Ba^{2+} and no added Ca^{2+}. The replacement of Ca^{2+} with Ba^{2+} alters the kinetics of tail current relaxations and removes initial rise in tail currents. It is likely that the ionic substitution reduces the contribution of Ca^{2+}-activated Cl^- currents. (D) Outward currents in Cx32N2E*Cx43E1 oocytes were elicited from a holding potential at −90 mV, with 30-s voltage steps ranging from 0 to +40 mV in 10-mV increments. Inward tail currents resulted from the repolarization of the membrane to −90 mV. The bath solutions contained 5 mM Ca^{2+}. At voltages exceeding +30 mV, currents plateau consistent with the reversal of gating polarity by the N2E substitution. The time constants of tail-current relaxations are substantially faster than those observed in Cx32*Cx43E1 conductive hemichannels. (Inset) Current traces elicited by positive voltage steps are expanded.

current levels (Fig. 2 B). The replacement of Ca^{2+} with 2 mM Ba^{2+} alters the shape and time course of the tail currents; notably the initial increase in tail currents is absent (Fig. 2 C). It is likely that the substitution of Ca^{2+} with Ba^{2+} reduces the contribution of Ca^{2+}-activated Cl^- currents that are endogenous to *Xenopus* oocytes (Weber, 1999). While other currents endogenous to oocytes may also contribute to the complex time course of tail-current relaxations, the results suggest that the gating of the Cx32*Cx43E1 conductive hemichannel is in itself complex and likely to reflect a multiplicity of channel states or different gating mechanisms.

A representative macroscopic recording of Cx32N2E*Cx43E1 conductive hemichannels in 5 mM Ca^{2+}-containing bath solutions is presented in Fig. 2 D. Unlike the hemichannels formed by the chimeric parental connexin, Cx32*Cx43E1, macroscopic currents plateau and decline at membrane potentials exceeding +30 mV. The decrease in macroscopic currents is consistent with the reversal of the gating polarity of Cx32N2E*Cx43E1 hemichannels in intercellular pairings (see Fig. 1).

*Single channel recordings of Cx32*Cx43E1 conductive hemichannels.* Cell-attached patch recordings of a single Cx32*Cx43E1 conductive hemichannel expressed in *Xenopus* oocyte membranes in divalent cation-free bath solutions are presented in Fig. 3. At the negative membrane potentials shown (the resting membrane potential in these experiments was typically between 0 and −10 mV), the Cx32*Cx43E1 conductive hemichannel flickers between levels that correspond to fully open and subconductance levels. In these recordings, the current corresponding to full closures can be determined by loop gating closures (see Fig. 5 B). The mean closed duration of the rapid "flickery" transitions is 1.5 ms at −70 mV (Fig. 3 B). The entry of the channel into this "short-duration" substate does not substantially reduce the open probability of the channel. The open probability of the channel is ∼0.90 at −80 mV when channel closures occur by this mechanism. At larger negative potentials, channel closures to longer-lived subconductance levels become evident (for example, in the −80-mV trace in Figs. 3 A and 4 A). The open probability of the channel shown in the longer current trace in Fig. 4 A is ∼0.57 at −80 mV. At moderate positive membrane potentials, the open probability of the channel approaches 1.0 (Fig. 3 A).

As illustrated in Fig. 4 A, the channel adopts a "bursting" behavior at negative potentials. While the frequency of "short-duration" events (1.5 ms closed duration) increases as the membrane is hyperpolarized, much longer-lived transitions to at least one subconductance level appear (Figs. 3 A and 4 A). The time that the channel resides at these longer-lived subconductance levels ranges from tens of milliseconds to tens of seconds. The events-list histogram of closures to substates of duration >50 ms at −80 mV, shown in Fig. 4 B, is well fit by a sum of two exponentials with time constants, τ_1 = 56.8 ms and τ_2 = 593 ms. Events with durations longer than 3 s become more prevalent as the oocyte membrane is hyperpolarized beyond −80 mV, but because the closures are of such long duration, we were unable to record a sufficient number of events to estimate their time constant. As described above, the reduction in open probability caused by the entry of the channel into these "longer-lived" (>50 ms duration) substates largely accounts for the decrease in junctional currents observed in macroscopic recordings of intercellular channels and to the relaxation of tail currents in conductive hemichannels formed by the Cx32*Cx43E1 chimera (Fig. 2). As discussed below, channel closures by loop gating have the same polarity and therefore are also likely to contribute to the tail currents observed at negative potentials.

Fig. 5 A demonstrates that the Cx32*Cx43E1 conductive hemichannel can also enter into at least two other subconductance levels at negative membrane potentials (−100 mV in the case shown).

The Cx32*Cx43E1 conductive hemichannel also undergoes loop gating at sufficiently large membrane negative voltages (Fig. 5 B, *). Loop gating transitions between the fully open and fully closed states are characterized by a series of stepwise reductions in conductance that give the overall appearance of "slow gating transitions." Loop gating closures become more prevalent at hyperpolarizing membrane potentials in both Cx46- and Cx32*Cx43E1 conductive hemichannels, although they are observed less frequently in cell-attached patches of Cx32*Cx43E1-expressing oocytes than those expressing Cx46 and tend to appear at more negative membrane potentials.

Similar complexities in kinetics and the existence of multiple subconductance levels (reflecting both V_j gating and loop gating) have been described in single-channel records of intercellular channels formed by Cx32 and Cx26 (see Oh et al., 1997, 1999). It is likely that the molecular determinants of gating in the Cx32*Cx43E1 conductive hemichannel are similar to those in intercellular channels formed by both Cx32 and Cx32*Cx43E1.

The behavior of a single Cx32*Cx43E1 conductive hemichannel at positive membrane potentials is illustrated in Fig. 5 C. Typically, the channel remains at the fully open conductance level when the membrane potential is less than +70 mV. However, at potentials greater than +70 mV, transitions to a single subconductance level are observed in long recordings. These transitions are infrequent and their polarity is opposite that of V_j gating and loop gating. It is likely that they are due to a third gating mechanism, and they may account for the slight

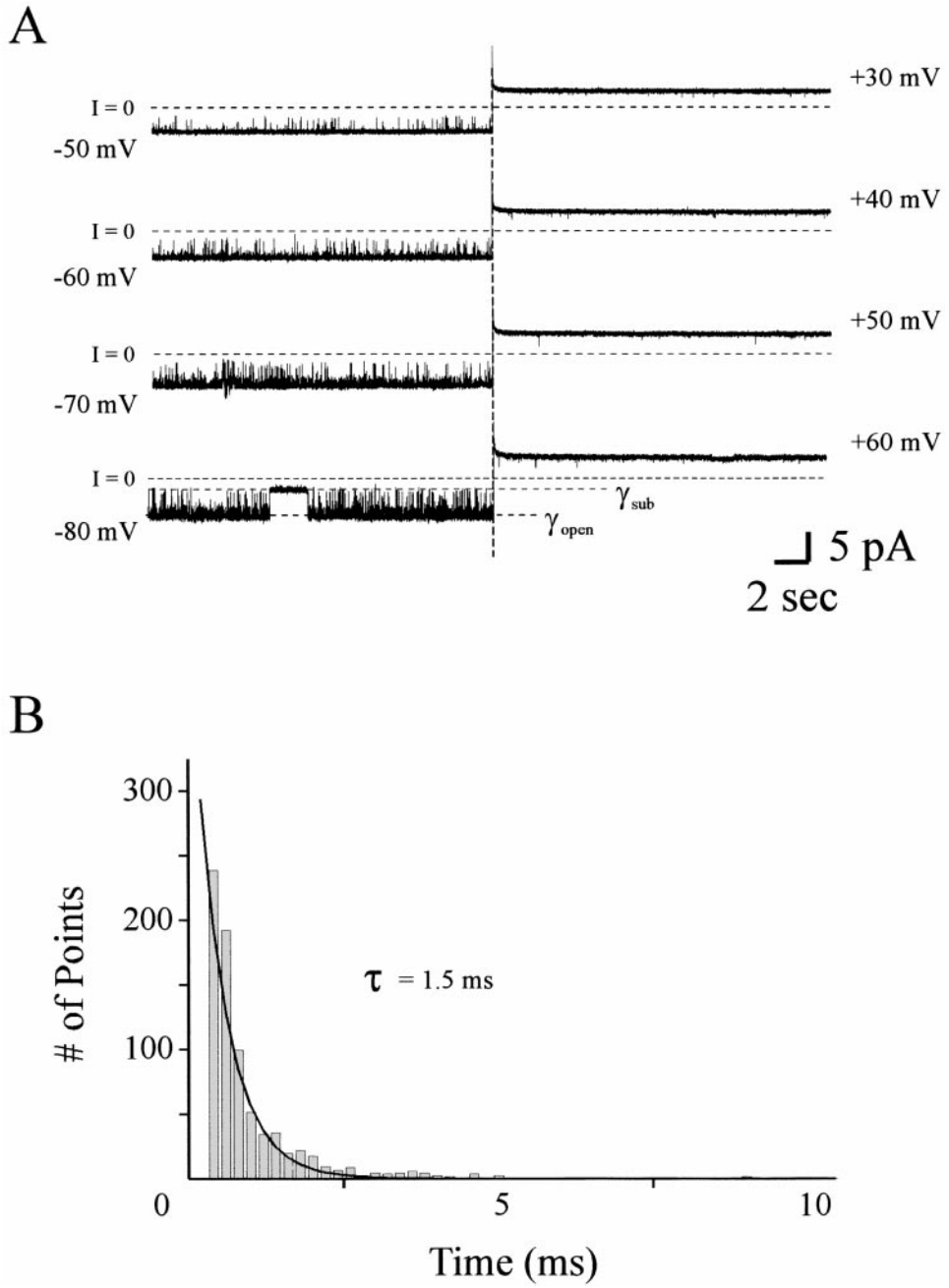

Figure 3. Voltage dependence of rapid gating transitions in single Cx32*Cx43E1 conductive hemichannels. (A) Cell-attached patch recordings of a single Cx32*Cx43E1 conductive hemichannel at different voltages, showing that the frequency of rapid transitions increases at larger hyperpolarizing potentials. The holding potential was flipped at the dotted vertical line from the hyperpolarizing to the depolarizing potential denoted. Leak currents were not subtracted. (B) An event list histogram of closed times at −70 mV. The histogram is best fit by a single exponential with a time constant, τ = 1.5 ms.

relaxation of junctional currents observed in the macroscopic recordings of the heterotypic Cx32*Cx43E1/Cx26 junction when the Cx26 cell is made relatively negative (Fig. 1 B). This third gating mechanism has the wrong polarity to account for the V_m dependence observed in Cx32*Cx43E1 homotypic junctions.

A comparison of the I-V relations of Cx32*Cx43E1 conductive hemichannels obtained with different voltage-ramp protocols is presented in Fig. 6. In ±100-mV ramps of short duration (3 s) from an initial holding potential of approximately −10 mV (the resting potential of the oocyte when Cx32*Cx43E1 conductive hemichannels are expressed), channel closures are observed only at negative membrane potentials and primarily involve gating transitions to subconductance levels (i.e., V_j gating) (Fig. 6, A and B). Transitions ascribable to loop gating are observed infrequently in current traces obtained with this voltage-ramp protocol. Channel closures to substates at positive membrane potentials are more likely to be observed in the I-V relations elicited by longer duration (8 s) voltage ramps (Fig. 6, C and D).

The inward rectification of open-channel currents seen in cell-attached records is also evident when ex-

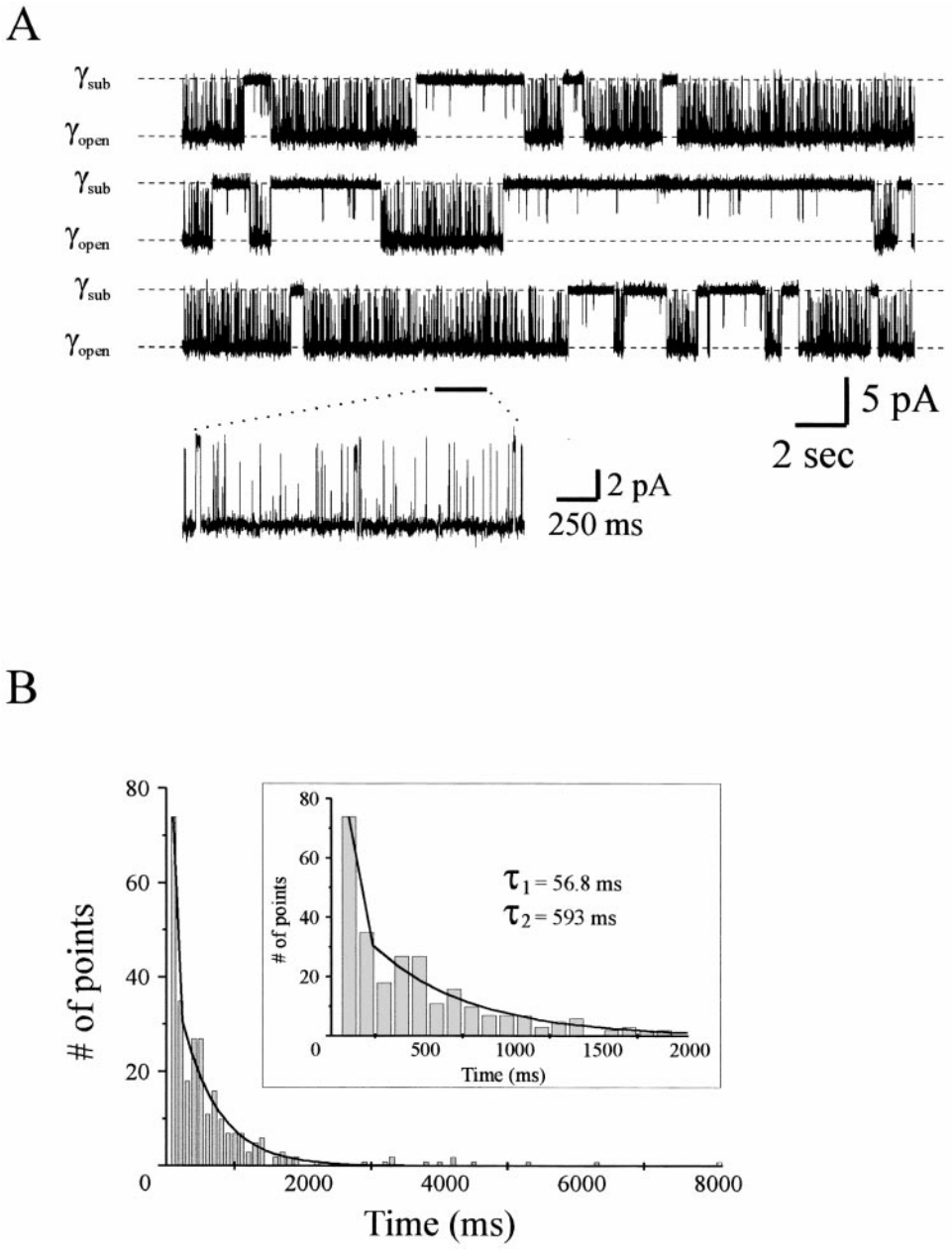

Figure 4. Voltage-dependent gating of a Cx32*Cx43E1 conductive hemichannel. (A) A cell-attached recording of a single Cx32*Cx43E1 conductive hemichannel at −80 mV. In addition to the rapid flickers (Fig. 3), the channel resides at longer-lived subconductance levels, with durations that range from tens of milliseconds (shown on expanded trace) to tens of seconds. (B) An event list histogram of closures with duration longer than 50 ms at −80 mV. The histogram is best fit by a double exponential with time constants, τ_1 = 56.8 ms and τ_2 = 593 ms. (Inset) The portion of the histogram from 0 to 2 s is shown.

cised patches are placed in symmetric (ND98) salt solutions (not shown). This result indicates that the open-channel rectification is likely to arise from an asymmetry in the position of fixed charges residing in or near the channel pore (see Oh et al., 1999). It does not arise solely from differences in the ionic composition of the oocyte cytoplasm and the patch recording solutions.

*Single channel recordings of Cx32N2E*Cx43E1 conductive hemichannels.* Cell-attached recordings of single Cx32N2E*Cx43E1 conductive hemichannels are shown in Fig. 7. In divalent cation-free solutions (Fig. 7, A–C), closures to subconductance levels are observed even at small positive membrane potentials (+20 mV). The voltage dependence of the open probability of homomeric Cx32N2E*Cx43E1 conductive hemichannels is presented in Fig. 8 B for positive membrane potentials. No gating events to subconductance levels are observed at negative membrane potentials. However, loop-gating transitions are still observed at negative membrane potentials (Fig. 7 C). Overall, these results are consistent with the macroscopic behavior of the Cx32N2E*Cx43E1 conductive hemichannel (Fig. 2 D). The shift in the voltage dependence of the Cx32*Cx43E1 conductive hemichannel caused by the N2E substitution is similar to that observed for both Cx32N2E and Cx32N2E*Cx43E1 hemichannels when either is paired to form homotypic and heterotypic intercellular channels with Cx26 and Cx32 (Fig. 1; Oh et al., 1999).

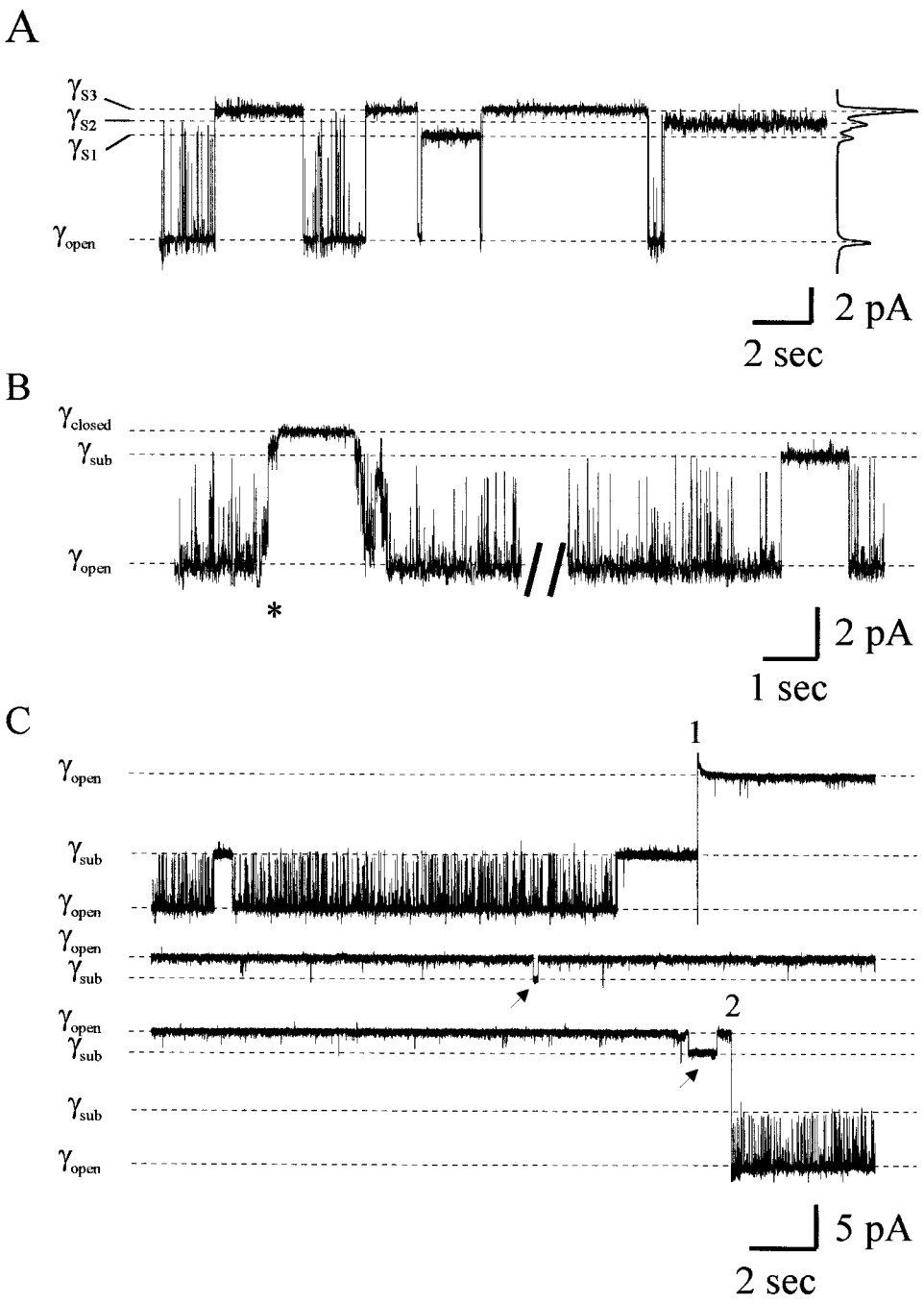

Figure 5. Single-channel recordings of Cx32*Cx43E1 conductive hemichannel illustrating three different gating mechanisms. (A) V_j gating is illustrated by the outside-out patch recording at −100 mV. The channel can enter one of three subconductance states denoted as S1, S2, and S3. An amplitude histogram of this trace is shown on the right side of record. Single channels in excised membrane patches are less stable than those of cell-attached patches. The basis for this difference is unknown. (B) A cell-attached patch recording of a single Cx32*Cx43E1 conductive hemichannel obtained at a holding potential of −70 mV. The channel undergoes a series of gating transitions (*) that may result in full closure, termed loop gating. (C) A cell-attached patch recording of a single Cx32*43E1 conductive hemichannel illustrating gating transitions to a subconductance level (arrows) at a depolarizing membrane potential of +80 mV (the section of the record between numerals 1 and 2). At positions 1 and 2, the membrane potential was reversed from −80 to + 80 mV and from +80 to −80 mV, respectively. V_j gating events are evident in the portions of the current trace elicited by the hyperpolarization of the membrane to −80 mV. Leak currents were not subtracted.

Interestingly, the N2E substitution causes a substantial change in the I-V relation of the fully open Cx32*Cx43E1 conductive hemichannel. As illustrated in Fig. 7 D, there is a slight outward rectification of currents. The change in rectification most likely reflects the effect of the negative charge of the glutamic acid residue, which should be located near the cytoplasmic end of the channel. A comparable I-V relation to that observed can be obtained with the application of the 1-D Poisson-Nernst-Plank model of Chen and Eisenberg (1993) using a charge distribution model based on those described for Cx32N2E intercellular channels by Oh et al. (1999) (not shown).

Stoichiometry of V_j Gating Polarity Reversal by the N2E Substitution

The behavior of single heteromeric conductive hemichannels, formed by coinjecting RNA synthesized from mixtures of Cx32*Cx43E1 and Cx32N2E*Cx43E1 DNA templates is shown in Fig. 8 A. Single heteromeric conductive hemichannels containing mixtures of Cx32N2E*Cx43E1 and Cx32*Cx43E1 are bipolar; that

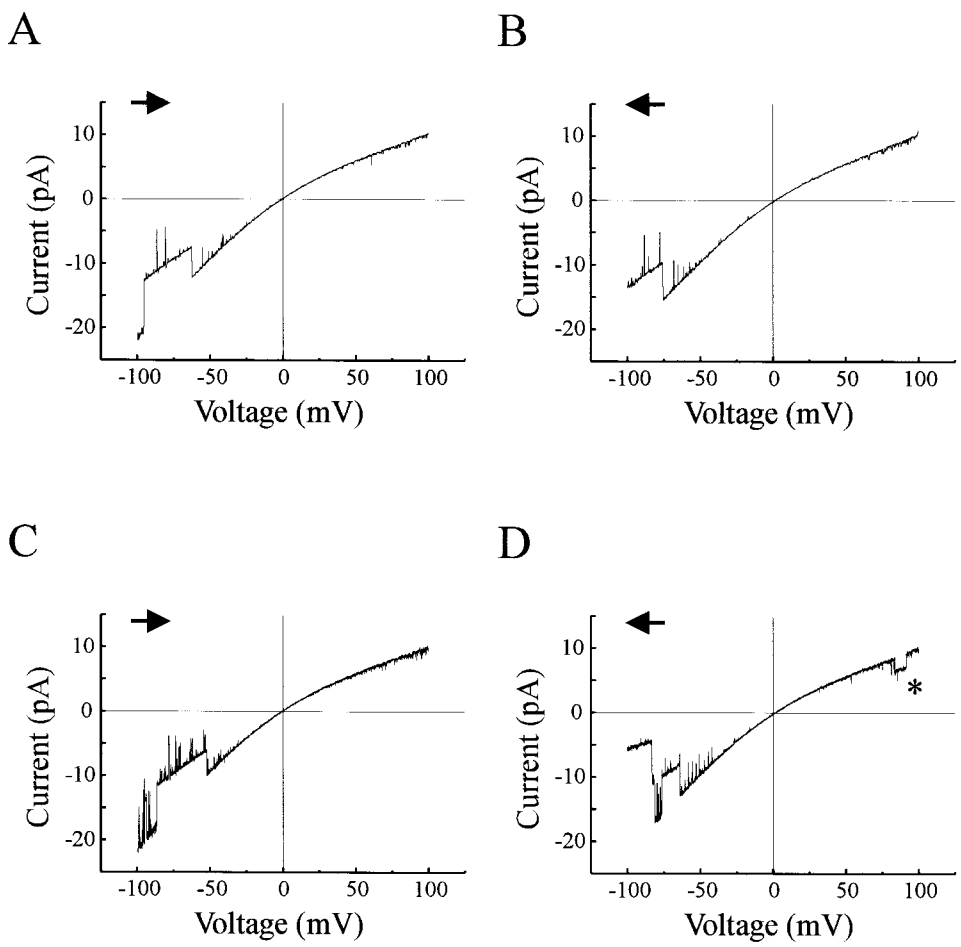

Figure 6. Current–voltage relations of Cx32*Cx43E1 conductive hemichannels obtained by the application of ±100-mV ramps in a cell-attached patch configuration. Arrows indicate the direction of the time axis. In A and C, voltage was ramped from −100 to +100 mV, in B and D from +100 to −100 mV. In the 3-s-duration voltage ramps shown in A and B, current rectifies inwardly and the channel closes to subconductance levels only at hyperpolarizing potentials. The overall form of the I-V relation elicited by the positive going ramp shown in A is similar to that elicited by the negative going ramp shown in B. (C and D) In 8-s voltage ramps, an additional gating transition (*) is observed at depolarizing potentials (see Fig. 5 C). The baseline currents were adjusted to zero in these records. The records were digitally filtered at 200 Hz for presentation.

is, they can close to subconductance levels at both positive and negative membrane potentials, but remain open at membrane potentials around zero. This is most easily seen in the I-V relation shown in Fig. 8 C. This contrasts the behavior of homomeric Cx32N2E*Cx43E1 conductive hemichannels, which close to subconductance levels only at positive membrane potentials. The observed bipolarity cannot be explained by a shift in voltage dependence resulting from a change in the chemical free energy of the channel, as closures are less frequent at membrane potentials around zero than at both larger positive and negative membrane potentials.

To define the subunit stoichiometry of V_j gating, we determined the distribution of gating polarities of single conductive hemichannels expressed in oocytes after injection with 20:1 and 1:20 RNA mixtures. In these experiments, the ratio of RNA is defined by the concentration of Cx32N2E*Cx43E1 compared with Cx32*Cx43E1. If both RNAs are expressed equally and the resulting protein subunits are assembled randomly into hexameric hemichannels, then the distribution of conductive hemichannel types will be predicted by the binomial distribution. In the 20:1 RNA mixture, 26.5% of channels should contain at least one Cx32*Cx43E1 subunit. In the 1:20 RNA mixture, 26.5% of channels should contain at least one Cx32N2E*Cx43E1 subunit. If the movement of a single appropriately charged subunit is sufficient to initiate V_j gating, then 26.5% of single conductive hemichannels are expected to display bipolar gating. If, however, at least two identical subunits are required, then only 3.28% of single conductive hemichannels are expected to display bipolar gating.

The symmetry of the binomial distribution provides a means of assessing the assumptions of equal efficacy of RNA translation and random assembly of mutant and wild-type subunits into hexameric conductive hemichannels. If all these assumptions are met, the ratio of bipolar to unipolar channels observed in 20:1 mixtures should be the same as that observed in 1:20 mixtures.

In 20:1 RNA mixtures of Cx32N2E*Cx43E1: Cx32*Cx43E1, 12 of 57 single conductive hemichannels observed (21.1%) displayed bipolar V_j gating similar to that illustrated in Fig. 8 A, top. The remainder of conductive hemichannels (78.9%) were indistinguishable from channels obtained when only Cx32N2E*Cx43E1 RNA was injected. The distribution of channel types observed does not differ significantly from that predicted by binomial distribution if one

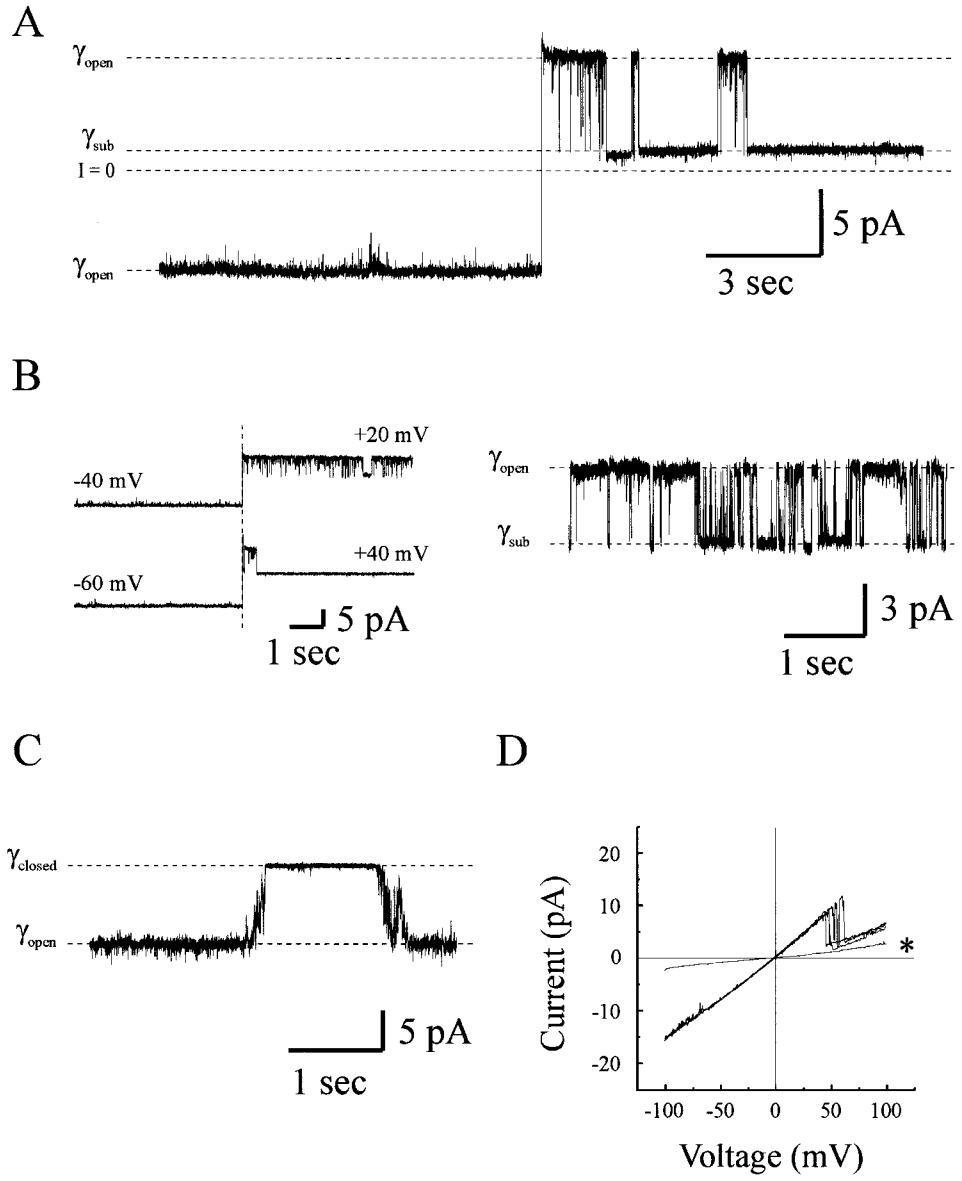

Figure 7. Single-channel recordings from *Xenopus* oocytes expressing Cx32N2E*Cx43E1 conductive hemichannels. (A) Cell-attached recording of a single Cx32N2E*Cx43E1 conductive hemichannel shows that the channel remains in a fully open state (−50 mV) and gates only upon depolarization (+50 mV). Leak currents were not subtracted. (B) The steepness of the voltage dependence of Cx32N2E*Cx43E1 conductive hemichannels is illustrated. The open probability of the channel decreases considerably over the 20-mV increment (+20 to +40 mV) shown (left). (Right) The open probability is intermediate at +30 mV. (C) A portion of a cell-attached record showing a loop gating event at a membrane potential of −60 mV. (D) The current–voltage relation of a single Cx32N2E*Cx43E1 conductive hemichannel obtained with 3-s voltage ramps from −100 to +100 mV in a cell-attached patch recording configuration. Four sequential current traces are superimposed. V_j-gating transitions are observed only at depolarizing potentials. Currents passing through the fully open state rectify outward slightly in contrast to the inward rectifying currents observed for Cx32*Cx43E1 conductive hemichannels. *The leak current of the patch. Baseline currents were adjusted to 0 pA. Current traces were digitally filtered at 200 Hz for presentation.

Cx32*Cx43E1 subunit is sufficient to cause bipolar gating ($\chi^2 = 0.015$, $P < 0.90$). We conclude that the single Cx32*Cx43E1 subunit is sufficient to initiate V_j gating at negative membrane potentials.

In oocytes injected with 1:20 mixtures of Cx32N2E*Cx43E1:Cx32*Cx43E1 RNA, 82 of 121 (67.8%) display behavior indistinguishable from conductive hemichannels formed by Cx32*Cx43E1. That is, these hemichannels close to subconductance levels at negative membrane potentials and transit to a subconductance level at positive membrane potentials exceeding 70 mV. The remaining conductive hemichannels (39 of 121, or 32.2%) display two distinct sets of transitions at depolarizing membrane potentials (Fig. 8 A, middle and bottom). At positive membrane potentials, transitions are observed that are comparable with those observed in the parental Cx32*Cx43E1 homomeric conductive hemichannel described above. This gating is exemplified by the transition in Fig. 8 A, *. The second population of gating transitions to subconductance levels have a substantially larger amplitude (Fig. 8 A, middle and bottom) and occur more frequently at smaller depolarizing membrane potentials (not illustrated). The distribution of conductive hemichannel types observed in 1:20 RNA mixtures does not differ significantly from that predicted by the binomial distribution if one N2E subunit is sufficient to cause bipolar gating ($\chi^2 = 0.017$, $P < 0.80$). We conclude that a single Cx32N2E*Cx43E1 subunit is sufficient to initiate channel closure at positive membrane potentials.

The slight asymmetry observed in the number of bipolar conductive hemichannels observed after injec-

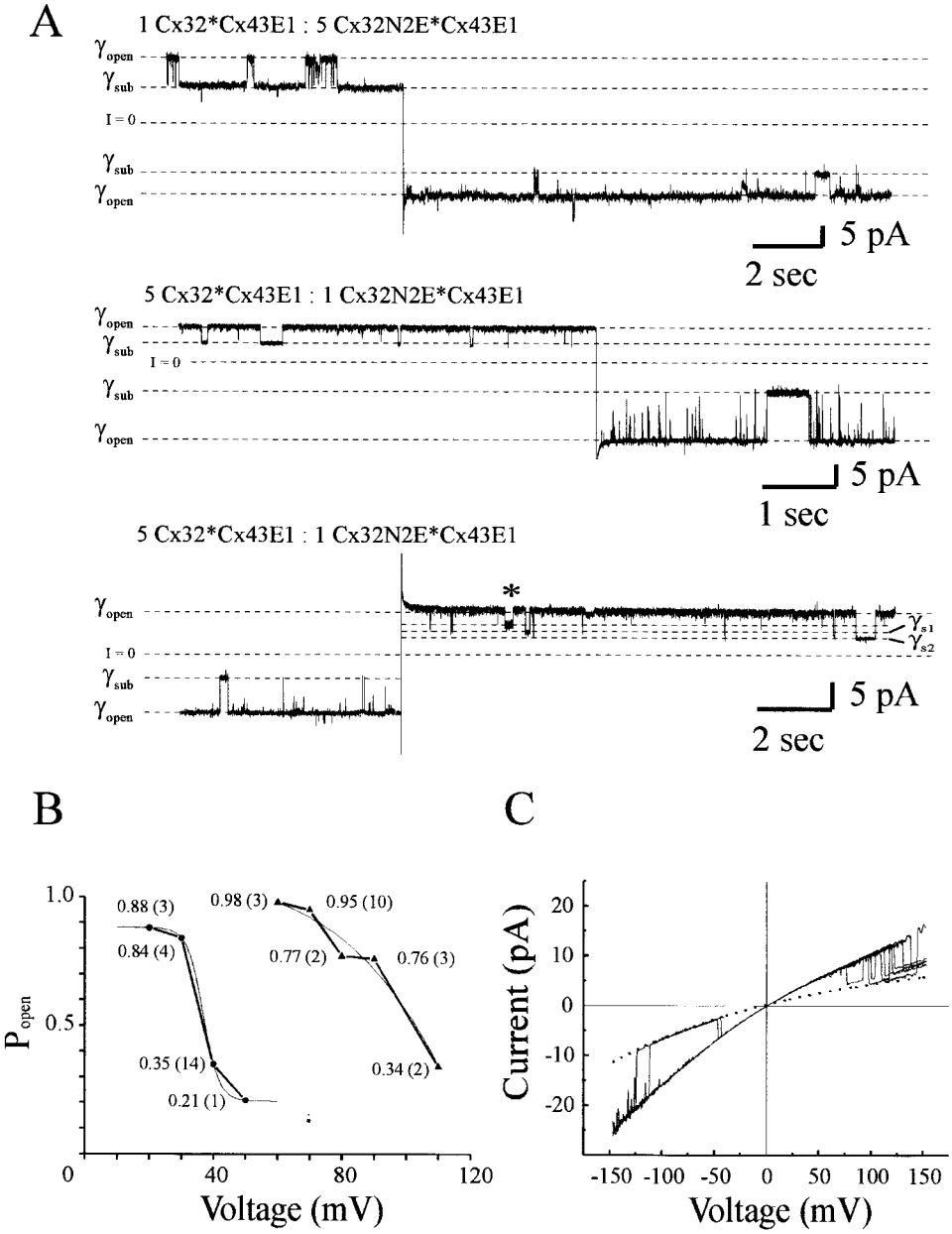

Figure 8. V_j gating of a heteromeric conductive hemichannels containing both Cx32*Cx43E1 and Cx32N2E*Cx43E1 subunits. (A) The cell-attached records illustrate that V_j gating is bipolar. The heteromeric hemichannel containing a single Cx32*Cx43E1 subunit makes transitions between fully open and subconductance levels at both positive and negative potentials (+50 and −80 mV, top). The heteromeric hemichannel containing a single Cx32N2E*Cx43E1 subunit makes transitions between fully open and subconductance levels at both positive and negative holding potentials (−120 and +80 mV, middle). (Bottom) The V_j-gating transitions to the two subconductance levels (S1 and S2) at depolarizing potential (+80 mV) are attributable to the presence of a single Cx32N2E*Cx43E1 subunit. The smaller amplitude transition (*, bottom) is attributable to a voltage-dependent process also observed in homomeric Cx32*Cx43E1 conductive hemichannels at depolarizing membrane potentials exceeding +70 mV (Fig. 5 C). Leak currents were not subtracted. (B) The open probability–voltage relation of homomeric Cx32N2E*Cx43E1 conductive hemichannel (●) and heteromeric conductive hemichannel containing a single Cx32N2E*Cx43E1 subunit (▲) are shown. The open probabilities of each channel are plotted as a function of holding potential. Open probabilities were calculated from the ratio of the areas under the peaks of all-point histograms. The numbers in parentheses are the numbers of different records that were concatenated and used to generate the all-point histograms at each voltage. The thin lines are fits of the data points to a Boltzmann relation with Microcal Origin 4.0 software. (C) Current–voltage relation of single heteromeric conductive hemichannel (containing one Cx32N2E*Cx43E1 and five Cx32*Cx43E1 subunits) obtained in a cell-attached configuration with 3-s voltage ramps from −150 to +150 mV. Four current traces from the same single channel record are superimposed. The heteromeric hemichannel gates between fully open and subconductance levels at both positive and negative potentials are shown. The dotted line is an exponential fit to the subconductance levels at negative potentials. The failure of the fitted curve to intersect the I-V relation of the substates at positive potentials illustrates that the channel substates observed at negative potentials do not correspond to the substates observed at positive potentials. The baseline current was adjusted to 0 pA and current traces were digitally filtered at 200 Hz for presentation.

tion of 20:1 and 1:20 RNA ratios (21.1 and 32.2%, respectively) can be explained if the Cx32N2E*Cx43E1 subunit was present in a slight excess relative to Cx32*Cx43E1. This may have been due to systematic error in the determination of the concentration of DNA templates used to synthesize RNA (see materials and methods). Alternatively, it may reflect a preferential rate of transcription or translation of the Cx32N2E*Cx43E1 construct, or a nonrandom assembly of the different subunits into hexameric hemichannels. However, the difference observed with the two RNA ratios does not alter the conclusion that a single appropriately charged subunit is sufficient to initiate V_j gating. If more than a single appropriately charged

subunit were required to the reverse gating polarity of a hexameric hemichannel, then no more than 3.28% of channels would be expected to exhibit bipolar gating behavior in either 20:1 or 1:20 RNA mixtures. This is far less than the number observed.

The open probabilities of homomeric Cx32N2E*Cx43E1 conductive hemichannels and heteromeric conductive hemichannels containing at least one Cx32N2E*Cx43E1 subunit are plotted as a function of positive membrane potential in Fig. 8 B. The observed open probability of the homomeric hemichannel is much less than that of the heteromeric hemichannel at comparable voltages. Also, the slope of the relation is steeper for the homomeric hemichannel. For simplicity, the changes in open probability at negative membrane potentials are not shown in Fig. 8 B. Note, however, that in the case of the homomeric Cx32N2E*Cx43E1 hemichannel, a reduction in open probability at large negative voltages should result as a consequence of loop gating. While in the case of the heteromeric hemichannel shown, the reduction in open probability that would be evident at negative potentials should result from V_j gating as well as loop gating. V_j gating would be initiated by any of the five Cx32*Cx43E1 subunits.

The I-V relations shown in Fig. 8 C illustrate two additional properties of the voltage gating of heteromeric conductive hemichannels that contain a single N2E subunit. First, it is apparent that a heteromeric hemichannel containing a single N2E subunit can make transitions to more than a single subconductance level at positive membrane potentials. This result indicates that the existence of multiple substates is not necessarily related to the number of subunits that are available to close for a given polarity of voltage. Second, the extrapolation of the I-V relation of the subconductance state that the hemichannel entered at negative membrane potentials (Fig. 8 C, dotted line) does not correspond to the I-V relation of any of the subconductance levels entered into at positive potentials. This result suggests that the conformations of the substates of the heteromeric hemichannel differ when closure is initiated by the movement of the single N2E subunit than when initiated by one of the five Cx32*Cx43E1 subunits.

Finally, it is interesting to note the presence of a single N2E subunit reduces the inward rectification of currents passing through the open state of the conductive hemichannel relative to that of the parental Cx32*Cx43E1 conductive hemichannel (compare Fig. 8 C with Fig. 6). Typically, open hemichannel currents with a single N2E subunit rectify ~1.5-fold over ±100 mV, compared with ~2-fold for the homomeric Cx32*Cx43E1 hemichannel over this voltage range. This result supports the conclusion that charges in the amino terminus lie within the channel pore and play a substantial role in ionic permeation of channels formed by these connexins (see Oh et al., 1999)

Description of a Channel Endogenous to Xenopus Oocytes

Single-channel records of the channels described above are often "contaminated" by an endogenous channel that is commonly found in *Xenopus* oocytes and may be mistaken for exogenously expressed conductive hemichannels formed by connexins. The endogenous *Xenopus* oocyte channel has a conductance of 20–25 pS at 30 mV and 30 pS at −50mV (Fig. 9 A). The channel becomes active at depolarizing membrane potentials and displays "use dependence," in that its activity at a given hyperpolarizing membrane potential is greater when the hyperpolarizing step is preceded by a membrane depolarization (Fig. 9 B). The open probability of the channel appears to decrease as a function of time at hyperpolarizing membrane potentials (Fig. 9 B), suggestive of a "rundown" mechanism. Another interesting feature of the channel is the long delay in channel reopening that is observed when the membrane potential is reversed from −90 to +90 mV (Fig. 9 B). The I-V relation of the open state of this channel is essentially linear (Fig. 9 C). Overall, the channel displays voltage-gating properties that are similar to mechanosensitive channels in *Xenopus* oocytes described by Gil et al. (1999) and to the depolarization-induced endogenous sodium conductance in *Xenopus* oocytes described by Kado and Baud (1981) and Rettinger (1999). However, the single channel conductance of the endogenous channel observed in cell-attached patches in our study is substantially greater than the <1-pS conductance that was predicted by Rettinger (1999) for the depolarization-induced sodium conductance, and the channel has appreciable permeability to both Na^+ and K^+ (E.B. Trexler, personal communication). Thus, the endogenous channel we describe is most likely the mechanosensitive channel. Other channels endogenous to *Xenopus* oocytes are also observed in divalent cation-free solutions (not shown), but they appear much less frequently than the channel described above and are more easily distinguished from conductive hemichannels formed by some connexins.

DISCUSSION

The major aim of this paper was to further elucidate the mechanism of transjunctional voltage gating by determining the stoichiometry of polarity reversal by a negative charge substitution (N2E) in the amino terminus of a Cx32 chimera (Cx32*Cx43E1). This chimera forms both intercellular channels and conductive hemichannels in *Xenopus* oocytes. This property has allowed us to compare the gating polarity of hemichannels paired to form intercellular channels with that of un-

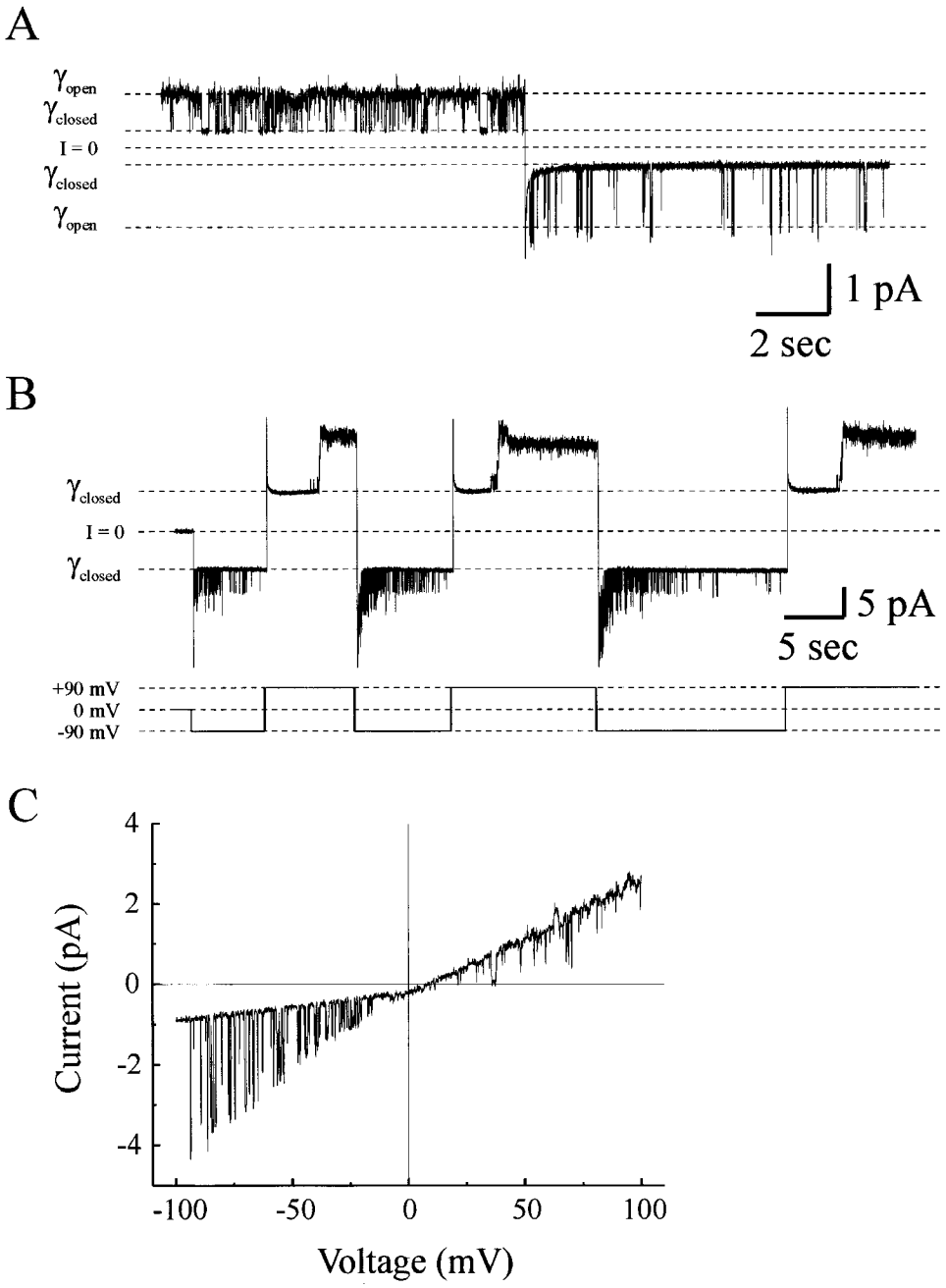

Figure 9. Cell-attached patch recordings of a nonconnexin channel endogenous to *Xenopus* oocytes. (A) A record of a single channel at a holding potential of +30 and −50 mV. The channel has a unitary conductance of 20–25 pS at +30 mV and 30 pS at −50 mV. (B) Currents elicited by alternating ±90-mV voltage steps. The channels are slowly activated by depolarization (+90 mV). At hyperpolarizing membrane potentials (−90 mV), the activated channels close and appear to run down. (C) The current–voltage relation of the endogenous *Xenopus* oocyte channel resulting from a 3-s voltage ramp from +100 to −100 mV. Baseline currents were not adjusted.

apposed hemichannels (conductive hemichannels) and to determine the stoichiometry of polarity reversal.

In our previous studies, we demonstrated that the polarities of V_j dependence of homomeric hemichannels formed by two Group I connexins, Cx26 and Cx32, are opposite when they are paired to form intercellular channels in *Xenopus* oocytes (Verselis et al., 1994). Cx32 homomeric hemichannels close at negative V_j, while Cx26 homomeric hemichannels close at positive V_j. The difference in polarity of V_j dependence of Cx32 and Cx26 hemichannels results from the electrostatic effect of a single charge difference located in the NH_2 terminus of the two connexins. Negative charge substitutions at the second position (Cx32N2D and Cx32N2E) reverse the gating polarity of Cx32 homomeric hemichannels while the complimentary substitution, Cx26D2N, reverses the gating polarity of Cx26 homomeric hemichannels.

The conclusions of our earlier study (Verselis et al., 1994) were based exclusively on macroscopic recordings of intercellular channels in pairs of *Xenopus* oocytes and tacitly assumed that V_j dependence arose by a single mechanism that was conserved in all connexin hemichannels. Subsequent single-channel studies dem-

onstrated the presence of two fundamentally distinct voltage-gating mechanisms in conductive hemichannels formed by Cx46 (Trexler et al., 1996) and in intercellular channels formed by Cx32 and Cx26 (Oh et al., 1997, 1999). One gating mechanism in homotypic and heterotypic intercellular channels formed by Cx26 and Cx32 is characterized by rapid transitions (submillisecond) between a fully open state and at least three distinct subconductance states in response to V_j. We reported that the polarity of the rapid gating transitions between open and subconductance states correlated with the opposite gating polarity of heterotypic Cx32/Cx26 channels and with the reversal of the polarity of V_j dependence by a negative charge substitution in the NH_2 terminus of Cx32 (see Oh et al., 1999). This mechanism is similar to that ascribed to V_j gating in Cx46 conductive hemichannels by Trexler et al. (1996). A second gating mechanism was also described in intercellular channels. This mechanism is characterized by a series of short-lived transitions that give the appearance of slow gating, similar in appearance to loop gating described in Cx46 conductive hemichannels by Trexler et al. (1996). Similar transitions have been observed during "docking/formation" studies of intercellular channels by Bukauskas et al. (1995). Transitions similar to loop gating are infrequent and observed at both polarities of V_j in single intercellular Cx32/Cx26 channels. They are more frequent in homotypic Cx32 and Cx26 intercellular channels (Oh et al., 1997, 1999).

In this paper, we demonstrate that Cx32*Cx43E1 homomeric conductive hemichannels close at negative V_j, as do wild-type Cx32 hemichannels in heterotypic pairings with Cx32 and Cx26 hemichannels and that the polarity of V_j dependence is reversed by the N2E substitution. We could not obtain stably transfected cell lines to examine the V_j-dependent gating of single homotypic and heterotypic intercellular channels formed by the chimera, but we infer that the mechanism is similar based on single-channel recordings of conductive hemichannels formed by Cx32*Cx43E1 and Cx32N2E*Cx43E1.

The results presented in this paper indicate that the mechanisms of voltage-dependent gating of Cx32*Cx43E1 conductive hemichannels are for the most part comparable with those of intercellular Cx32 channels described by Oh et al. (1999).

At negative potentials, the conductive hemichannel makes rapid transitions between the fully open state and closed substates (V_j gating) and "slow" (complex) transitions to the fully closed state (loop gating). Our results indicate that V_j gating of Cx32*Cx43E1 conductive hemichannels is complex; characterized by the presence of at least three distinct substates and at least four kinetically distinguishable substates with mean closed durations of $\sim$1.5, 55, 600, and $>$1,000 ms. The negative charge substitution, N2E, reverses the gating polarity of all these substates. The simplest interpretation of this result is that all of these gating events are initiated by, or result from, a conformational change in the NH_2 terminus.

The polarity of loop gating in Cx32*Cx43E1 conductive hemichannels is the same as that reported for Cx46 by Trexler et al. (1996). However, loop-gating transitions in Cx32*Cx43E1 conductive hemichannels are observed less frequently in cell-attached patch recordings and only occur at large negative membrane potentials. The ability of the N2E substitution to reverse the polarity of V_j gating but not loop gating in Cx32*Cx43E1 conductive hemichannels supports the conclusion that the two forms of gating are fundamentally distinct.

The closure of Cx32*Cx43E1 conductive hemichannels at positive membrane potentials exceeding +70 mV was unexpected as comparable closures are not observed in single channel records of heterotypic intercellular channels formed by Cx32 and Cx26, nor in Cx46 conductive hemichannels (see Trexler et al., 1996; Oh et al., 1999). This gating process may be unique to the Cx32*Cx43E1 conductive hemichannel and it is likely to represent a third distinct gating mechanism as the molecular determinants of this process are probably unrelated to the movement of the amino terminus. Recall that the N2E substitution, which reverses the polarity of V_j gating, does not appear to reverse the polarity of this voltage-dependent process. That is, no closures to subconductance levels are observed when the Cx32N2E*Cx43E1 conductive hemichannel is held at negative membrane potentials. However, it should be noted that the shift in the voltage dependence of V_j gating to small positive membrane potentials precludes the identification of these closures in the Cx32N2E*Cx43E1 conductive hemichannel. Therefore, we cannot exclude the possibility that the N2E substitution causes the loss of this process.

Stoichiometry of the Polarity Reversal of V_j Gating

The results presented in this study demonstrate that a single connexin subunit can initiate V_j gating. The bipolarity of heteromeric hemichannels containing oppositely charged NH_2 termini can be explained if the closures to substates that are observed at positive membrane potentials are initiated by the movement of an N2E subunit, while the closures to substates that are observed at negative potentials are initiated by the movement of a wild-type subunit. Thus, in effect, a hemichannel contains six voltage sensors, one in each subunit, that function individually but not necessarily independently to initiate V_j gating. This view is supported by all the available data.

Our results show that the voltage sensitivity of a hemichannel correlates with the number of appropriately charged subunits that are available to gate. In the case illustrated in Fig. 8 B, the probability that a Cx32N2E*Cx43E1 homomeric hemichannel (six identical subunits) closes at positive membrane potentials is substantially greater than that of a heteromeric hemichannel containing a single Cx32N2E*Cx43E1 subunit. This result can be explained if the open probabilities of heteromeric and homomeric hemichannels reflect the number of subunits that are available to initiate V_j gating. For example, in an independent gating model (no subunit interactions), the open probability of a homomeric hemichannel can be predicted from the binomial distribution using estimates of the probability that a single subunit of a heteromeric hemichannel will initiate V_j gating. If, for example, the open probability of a heteromeric hemichannel containing a single negatively charged subunit at a given positive voltage were 0.95, then the probability that all six subunits of a homomeric hemichannel formed by six negatively charged subunits would be open at the same voltage would be 0.74. However, the reduction in open probability that is observed at positive membrane potentials is much greater than predicted by a simple independent model (Fig. 8 B). For example, at voltages where the open probability of a heteromeric hemichannel containing a single N2E subunit is 0.95, the corresponding open probability of the homomeric N2E hemichannel is <0.2. The deviation from independence can be explained by postulating the existence of electrostatic interactions between subunits, which are likely to alter the free energy (stability) of the open and closed channel states. It is reasonable to expect that electrostatic attractions among oppositely charged subunits would stabilize the open state of a heteromeric hemichannel, while electrostatic repulsion among identically charged subunits would destabilize the open state of a homomeric hemichannel.

The difference in slope of the two open probability–voltage relations illustrated in Fig. 8 B is likely to reflect the movement of a greater amount of charge during voltage gating of the homomeric hemichannel than of the heteromeric hemichannel at positive potentials. A simple explanation for this observation is that, while the closure of the homomeric hemichannel in response to voltage may be initiated by the movement of the voltage sensor in a single subunit, ultimately all six subunits could move and contribute to the calculated gating charge. Whereas, in the heteromeric hemichannel, the slope of the relation may only reflect the movement of the charge contributed by the single N2E subunit. The possibility that multiple subunits respond to changes in membrane voltage may explain the multiexponential time course of current relaxations that is usually observed in macroscopic recordings of homomeric hemichannels at higher membrane potentials.

Allosteric Models of V_j Gating

While previous models have assumed that gating of intercellular channels (gap junctions) is likely to involve a concerted movement of all six connexin subunits (see, for example, Unwin, 1987; Bennett et al., 1991), the results presented in this paper favor an individual subunit gating model. The possibility that V_j gating requires the simultaneous movement of all six subunits (a concerted gating model, Fig. 10 A) seems unlikely. Consider for example the closure of a heteromeric hemichannel initiated by the movement of a single N2E subunit at positive membrane potentials. If closure were to occur by a concerted mechanism, then the voltage sensors of the five Cx32*Cx43E1 subunits would first have to move against, and then would be improperly oriented in the electric field. As this closed conformation should be energetically unfavorable, it is likely that the improperly oriented voltage sensors would realign in the electric field, causing the channel to reopen. Opening of the hemichannel would be strongly favored as it could be initiated by the movement of any one of the five Cx32*Cx43E1 subunits. Consequently, one would expect that closures of this heteromeric hemichannel at positive membrane potentials would be of very short duration. Visual inspection of the records presented in Fig. 8 A suggests that this is not the case. For example, the duration of closures initiated by the single N2E subunit (in the 5WT:1N2E heteromeric hemichannel) at positive potentials do not appear to be of substantially shorter duration than those initiated by the movement of one of the five positively charged Cx32*Cx43E1 subunits at negative potentials. If gating were to occur by a concerted mechanism, it would seemingly require that a conformational change take place in a separate domain of all six connexin subunits that would not depend on the position of the voltage sensor of a subunit. That is, the voltage sensor of any improperly oriented subunit would have to lie outside the field created by V_j when the subunit is forced to adopt a closed conformation. While this may be possible, it seems less likely than a simple individual subunit gating model like that illustrated in Fig. 10 B.

The I-V relation of the heteromeric conductive hemichannel presented in Fig. 8 C is also consistent with an individual gating model like that illustrated in Fig. 10 B. If gating resulted from a simple concerted mechanism, the set of substate conformations at negative potentials are likely to be the same as the set of substate conformations at positive potentials. This does not appear to be the case. Rather, the conformations of the "substates" of the hemichannel differ when closure is

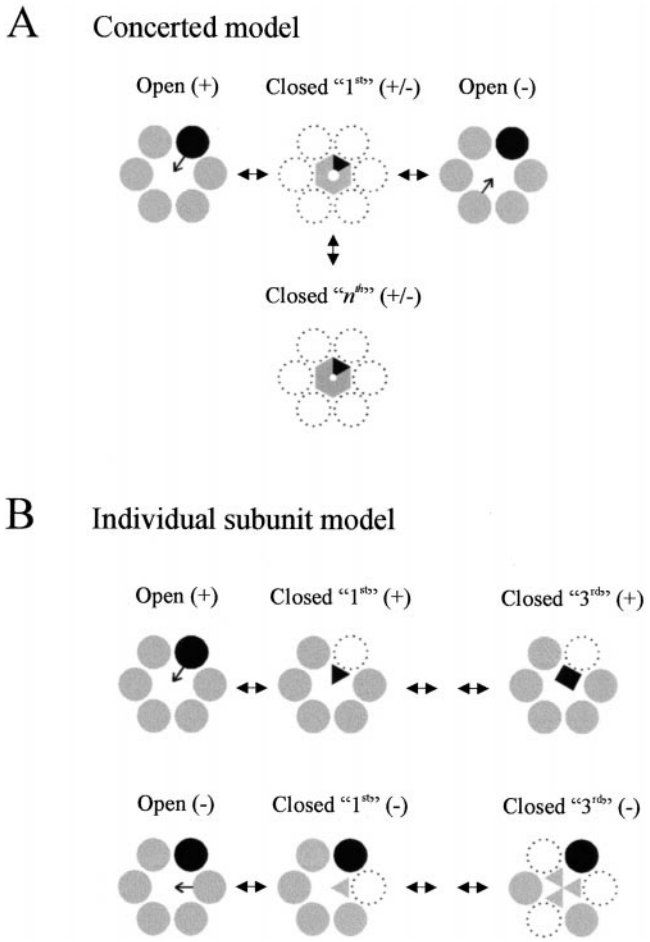

Figure 10. A comparison of concerted (A) and individual (B) subunit gating models for a heteromeric hemichannel containing a single N2E connexin subunit. In the concerted model shown in A, the movement of a voltage sensor in one subunit causes a similar conformational change in all six connexin subunits regardless of the orientation of their voltage sensors in the electric field. Substates arise by a concerted change in the conformation of all six subunits. The state depicted Closed "1st" (+/−) indicates that the channel enters the same substate in response to either membrane depolarization (+) or hyperpolarization (−). In the individual model shown in B, each subunit can respond autonomously to changes in the polarity of the electric field. Substates can result from changes in the conformation of one subunit, as illustrated (B, top) (in response to membrane depolarization, +) or by the changes in the conformation of multiple subunits as illustrated (bottom) (in response to membrane hyperpolarization, −). See text for details. Gray circle, positively charged subunit in an open conformation; solid circle, negatively charged subunit in an open conformation; gray triangle, positively charged subunit in a closed conformation; solid triangle, negatively charged subunit in a closed conformation; solid square, negatively charged subunit in another closed conformation.

initiated by an N2E-containing subunit than when closure is initiated by a Cx32*Cx43E1 subunit. The multiplicity of substates that arise from the movement of the single N2E-containing subunit, which is apparent in Fig. 8 C, suggests that a single subunit can adopt more than one "closed" conformation (see below).

Models of V_j Gating and Structural Implications

The ability of a single connexin subunit to initiate V_j gating suggests several refinements and additions to the models of V_j-dependent gating that we have previously proposed (Verselis et al., 1994; Ri et al., 1999). The major assertion underlying all V_j-gating models is that the V_j sensor and gate reside exclusively within a hemichannel (see Harris et al., 1981; Verselis et al., 1994). Our current results are consistent with and further support this view.

Previously, we suggested (Verselis et al., 1994) that the components of the voltage sensor are located in the NH_2 terminus and at the border of the first transmembrane segment (TM1) and first extracellular loop (E1) and postulated that the valence of the sensor is determined by the summation of charge at these positions across all six connexin subunits. This model arose partly from the observation that a charge substitution at the TM1/E1 border appeared to suppress the ability of N2E to reverse the gating polarity of Cx32. However, the demonstration that a single connexin subunit is sufficient to initiate V_j gating of heteromeric conductive hemichannels makes it unlikely that the valence of the voltage sensor is determined by the summation of charges. The simplest alternative model is that the V_j sensor resides exclusively in the NH_2 terminus of a connexin subunit and that the movement of charges located in the NH_2 terminus of a single subunit initiates the conformational changes that underlie V_j gating.

As discussed above, it is possible that both short- and long-range electrostatic interactions (such as among charges at the TM1/E1 border and NH_2 terminus) exist. However, these interactions appear limited to changing the likelihood that an individual subunit will respond to a given change in applied voltage, rather than determining the net valence of the voltage sensor and the likelihood that all six subunits will make a concerted transition. The ability of a charge substitution at the TM1/E1 border to suppress the reversal of Cx32 gating polarity by N2D can be explained if the TM1/E1 substitution caused a shift in the voltage dependence of loop gating that obscured the polarity of V_j gating. Thus, it is possible that the reversal of polarity by Cx32N2D was not suppressed by the charge substitution at the TM1/E1 border and consequently that charges at this position are not part of the V_j sensor.

The results presented in this paper demonstrate that V_j gating is complex and includes gating events of markedly different duration and the existence of several substates. The short duration closures (1.5 ms, Fig. 3), which are too brief to account for the current relax-

ations observed in macroscopic recordings of intercellular channels and conductive hemichannels formed by Cx32*Cx43E1 are likely to differ mechanistically from the longer duration closures (Fig. 4 B). Yet, as the gating polarities of both short- and long-duration events are reversed by the N2E substitution, they all must be related to movements of the NH_2 terminus. We propose that the NH_2 terminus is flexible and that the brief closures might reflect "local" changes in the conformation of the NH_2 terminus. We propose that the longer duration closures, which contribute more to the changes in conductance that are observed macroscopically, are initiated by another movement of the NH_2 terminus and are ultimately mediated by the dynamic properties of a proline kink motif found in the second transmembrane helix (P87 in Cx32) of all connexins (Ri et al., 1999).

Based on the molecular and computational studies described in Ri et al. (1999), we proposed that the movement of the connexin V_j sensor initiates a set of molecular changes in a connexin subunit that favor a reduction in the bend angle of the proline kink motif in the TM2 of Cx32. We proposed that this straightening of TM2 would displace TM1 and/or the NH_2 terminus into the channel pore (see Ri et al., 1999). The resulting reduction in pore radius would correspond to the entry of the channel into a subconductance state. The existence of multiple substates in heteromeric conductive hemichannels (5WT:1N2E) that are initiated by the single N2E subunit (Fig. 8 C) can be explained by an independent model if the proline kink motif in a given subunit were able to "ratchet" between different bend angles.

Finally, all individual gating models, such as the one depicted in Fig. 10 B, require that the interactions among the six subunits that form a hemichannel be sufficiently "elastic" to allow a single subunit to undergo conformational changes without forcing the adjacent subunits to adopt the same conformation. An explanation for how this may occur is suggested by the 3-D structure of a gap junction channel reported by Unger et al. (1999). The 7-Å resolution structure reveals that the two transmembrane helices that line the pore are packed with a right-handed twist, while the outer two helices are packed with a left-handed twist (Unger et al., 1999). It is possible that this arrangement minimizes interactions between the two pairs of transmembrane helices and consequently allows them to function individually. Our results can be explained if the conformational changes that underlie V_j gating are restricted to the inner pair of helices (which we believe are TM1 and TM2) and that these changes do not substantially perturb the conformation of the outer pair of helices (TM3 and TM4), nor that of the helices in the adjacent subunits.

The model that emerges from our studies is that the first and second transmembrane helices of each of the six connexin subunits interact to form a functional domain, which contributes to the formation of the channel pore and plays a central role in the mechanism of V_j gating. Our results indicate that the connexin V_j sensor resides in the NH_2 terminus and that the movement of the voltage sensor in a single connexin subunit is sufficient to initiate the set of conformational changes that result in channel closure to subconductance levels. We propose that hemichannel "closure" does not arise by a concerted mechanism but rather results from the changes in the conformation of individual subunits. Substates resulting from V_j gating may arise in two ways: a given subunit may adopt one of several different "closed conformations" and more than one subunit may adopt a closed conformation.

We thank Angele Bukauskiene and Joe Zavilowitz for technical assistance and Brady Trexler for his comments and permission to cite some of his unpublished work.

This work was supported by the National Institutes of Health grant GM 46889.

Submitted: 16 December 1999
Revised: 7 April 2000
Accepted: 11 April 2000

REFERENCES

Barrio, L.C., T. Suchyna, T. Bargiello, L.X. Xu, R.S. Roginski, M.V. Bennett, and B.J. Nicholson. 1991. Gap junctions formed by connexins 26 and 32 alone and in combination are differently affected by applied voltage. *Proc. Natl. Acad. Sci. USA.* 88:8410–8414.

Bennett, M.V.L., L.C. Barrio, T.A. Bargiello, D.C. Spray, E.L. Hertzberg, and J.C. Saez. 1991. Gap junctions: new tools, new answers, new questions. *Neuron.* 6:305–320.

Bukauskas, F.F., and R. Weingart. 1994. Voltage-dependent gating of single gap junction channels in an insect cell line. *Biophys. J.* 67:613–625.

Bukauskas, F.F., C. Elfgang, K. Willecke, and R. Weingart. 1995. Biophysical properties of gap junction channels formed by mouse connexin40 in induced pairs of transfected HeLa cells. *Biophys. J.* 68:2289–2298.

Bukauskas, F.F., and C. Peracchia. 1997. Two distinct gating mechanisms in gap junction channels: CO_2 sensitive and voltage sensitive. *Biophys. J.* 72:2137–2142.

Castro, C., J.M. Gomez-Hernandez, K. Silander, and L.C. Barrio. 1999. Altered formation of hemichannels and gap junction channels caused by C-terminal connexin-32 mutations. *J. Neurosci.* 19: 3752–3760.

Chen, D., and R. Eisenberg. 1993. Charges, currents and potentials in ionic channels of one conformation. *Biophys. J.* 64:1405–1421.

Ebihara, L., V.M. Berthoud, and E.C. Beyer. 1995. Distinct behavior of connexin56 and connexin46 gap junctional channels can be predicted from the behavior of their hemi-gap-junctional channels. *Biophys. J.* 68:1796–1803.

Ebihara, L. 1996. Xenopus connexin38 forms hemi-gap-junctional channels in the nonjunctional plasma membrane of *Xenopus* oocytes. *Biophys. J.* 71:742–748.

Gil, Z., K.L. Magelby, and S.D. Silberberg. 1999. Membrane-pipette interactions underlie delayed voltage activation of mechanosensitive channels in *Xenopus* oocytes. *Biophys. J.* 76:3118–3127.

Harris, A.L., D.C. Spray, and M.V. Bennett. 1981. Kinetic properties of a voltage-dependent junctional conductance. *J. Gen. Physiol.* 77:95–117.

Hertzberg, E.L., R.M. Disher, A.A. Tiller, Y. Zhou, and R.G. Cook. 1988. Topology of the Mr 27,000 liver gap junction protein. Cytoplasmic localization of amino- and carboxyl termini and a hydrophilic domain which is protease-hypersensitive. *J. Biol. Chem.* 263: 19105–19111.

Kado, R.T., and C. Baud. 1981. The rise and fall of electrical excitability in the oocyte of *Xenopus laevis. J. Physiol.* 77:1113–1117.

Lazark, A., and C. Peracchia. 1993. Gap junction gating sensitivity to physiological internal calcium regardless of pH in Novikoff hepatoma cells. *Biophys. J.* 65:2002–2012.

Milks, L.C., N.M. Kumar, R. Houghten, N. Unwin, and N.B. Gilula. 1988. Topology of the 32-kd liver gap junction protein determined by site-directed antibody localizations. *EMBO (Eur. Mol. Biol. Organ.) J.* 7:2967–2975.

Neyton, J., and A. Trautmann. 1985. Single channel currents of an intercellular junction. *Nature.* 317:331–335.

Oh, S., Y. Ri, M.V.L. Bennett, E.B. Trexler, V.K. Verselis, and T.A. Bargiello. 1997. Changes in permeability caused by connexin 32 mutations underlie X-linked Charcot-Marie-Tooth disease. *Neuron*. 19:927–938.

Oh, S., J.B Rubin, M.V.L. Bennett, V.K. Verselis, and T.A. Bargiello. 1999. Molecular determinants of electrical rectification of single channel conductance in gap junctions formed by connexins 26 and 32. *J. Gen. Physiol.* 114:339–364.

Paul, D.L., L. Ebihara, L.J. Takemoto, K.I. Swenson, and D.A. Goodenough. 1991. Connexin46, a novel lens gap junction protein, induces voltage-gated currents in nonjunctional plasma membrane of *Xenopus* oocytes. *J. Cell Biol.* 115:1077–1089.

Rettinger, J. 1999. Novel properties of the depolarization-induced endogenous sodium conductance in the *Xenopus laevis* oocyte. *Pflügers Arch.* 437:917–924.

Ri, Y., J.A. Ballesteros, C.K. Abrams, S. Oh, V.K. Verselis, H. Weinstein, and T.A. Bargiello. 1999. The role of a conserved proline residue in mediating conformational changes associated with voltage gating of Cx32 gap junctions. *Biophys. J.* 76:2887–2898.

Rubin, J.B., V.K. Verselis, M.V.L. Bennett, and T.A. Bargiello. 1992. Molecular analysis of voltage dependence of heterotypic gap junctions formed by connexins 26 and 32. *Biophys. J.* 62:183–195.

Trexler, E.B., M.V.L. Bennett, T.A. Bargiello, and V.K Verselis. 1996. Voltage gating and permeation in a gap junction hemichannel. *Proc. Natl. Acad. Sci. USA.* 93:5836–5841.

Trexler, E.B., F.F. Bukauskas, M.V.L. Bennett, T.A. Bargiello, and V.K. Verselis. 1999. Rapid and direct effects of pH on connexins revealed by the Cx46 hemichannel preparation. *J. Gen. Physiol.* 113:721–742.

Unger, V.M., N.M. Kumar, N.B. Gilula, and M. Yeager. 1999. Three dimensional structure of a recombinant gap junction membrane channel. *Science.* 283:1176–1180.

Unwin, P.N. 1987. Gap junction structure and the control of cell-to-cell communication. *Ciba Found. Symp.* 125:78–91.

Veenstra, R.D. 1996. Size and selectivity of gap junction channels formed from different connexins. *J. Bioenerg. Biomembr.* 28:327–337.

Verselis, V.K., M.V.L. Bennett, and T.A. Bargiello. 1991. A voltage-dependent gap junction in *Drosophila melanogaster. Biophys. J.* 59: 114–126.

Verselis, V.K., C.S. Ginter, and T.A. Bargiello. 1994. Opposite voltage gating polarities of two closely related connexins. *Nature.* 368:348–351.

Weber, W.M. 1999. Endogenous ion channels in oocytes of *Xenopus laevis*: recent developments. *J. Membr. Biol.* 170:1–12.

Zimmer, D.B., C.R. Green, W.H. Evans, and N.B. Gilula. 1987. Topological analysis of the major protein in isolated intact rat liver gap junctions and gap junction-derived single membrane structures. *J. Biol. Chem.* 262:7751–7763.